Searching for a charged Higgs boson with both $H^{\pm}W^{\mp}Z$ and $H^{\pm}tb$ couplings at the LHC

Jian-Yong Cen,[a] **Jung-Hsin Chen,**[b] **Xiao-Gang He,**[c,b,d] **Gang Li,**[b] **Jhih-Ying Su**[b] **and Wei Wang**[e]

[a] *School of Physics and Information Engineering, Shanxi Normal University,*
 Linfen, Shanxi 041004, China
[b] *Department of Physics, National Taiwan University,*
 Taipei 10617, Taiwan
[c] *Tsung-Dao Lee Institute & SKLPPC,*
 School of Physics and Astronomy, Shanghai Jiao Tong University,
 800 Dongchuan Rd., Shanghai 200240, China
[d] *Physics Division, National Center for Theoretical Sciences,*
 Hsinchu 30013, Taiwan
[e] *INPAC, SKLPPC, School of Physics and Astronomy, Shanghai Jiao Tong University,*
 800 Dongchuan Rd., Shanghai 200240, China
 E-mail: cenjy@sxnu.edu.cn, lewis02030405@gmail.com,
 hexg@phys.ntu.edu.tw, gangli@phys.ntu.edu.tw, b02202013@ntu.edu.tw,
 wei.wang@sjtu.edu.cn

ABSTRACT: In certain new physics scenarios, a singly charged Higgs boson can couple to both fermions and $W^{\pm}Z$ at tree level. We develop new strategies beyond current experimental searches using $pp \to jjH^{\pm}$, $H^{\pm} \to tb$ at the Large Hadron Collider (LHC). With the effective $H^{\pm}W^{\mp}Z$ and $H^{\pm}tb$ couplings we perform a model-independent analysis at the collision energy $\sqrt{s} = 13\,\text{TeV}$ with the integrated luminosity of 3 ab^{-1}. We derive the discovery prospects and exclusion limits for the charged Higgs boson in the mass range from 200 GeV to 1 TeV. With $|F_{WZ}|, |A_t| \sim 0.5$–1.0 and 300 GeV $\lesssim m_{H^{\pm}} \lesssim 400$ GeV, we point out that a discovery significance of 5σ can be achieved. The constraints and projected sensitivities are also discussed in a realistic model, i.e., the modified Georgi-Machacek model without custodial symmetry. Our proposed search would provide direct evidence for a charged Higgs boson $H^{\pm}$ that couples to $W^{\pm}Z$ and tb, and has better sensitivity to the couplings of $H^{\pm}W^{\mp}Z$ and $H^{\pm}tb$ than current searches.

Contents

1 Introduction

The discovery of the Higgs boson with a mass around 125 GeV [1, 2] at the Large Hadron Collider (LHC) has provided much information on electroweak symmetry breaking (EWSB) and particle mass generation. All available measurements of the couplings of the Higgs boson [3–5] are consistent with standard model (SM) with a minimal scalar sector of one Higgs doublet H. In the SM, H transforms under the electroweak gauge group $\mathrm{SU}(2)_L \times \mathrm{U}(1)_Y$ as $(2, -1/2)$,[1] and can be written as $H = ((v_H + h + iI_H)/\sqrt{2}, h^-)^T$. The non-zero vacuum expectation value (VEV) v_H is the source to induce the EWSB and generate the mass. $h^{\pm}$ and I_H are "eaten" by $W^{\pm}$ and Z boson as their longitudinal components and therefore only h is a physical Higgs boson. Is the Higgs boson discovered by the LHC really the one in the SM or does it have new interactions? Are there additional Higgs bosons? These are important questions in particle physics today.

In models extended with additional Higgs multiplets, one can achieve a richer particle spectrum in the scalar sector. By adding a $\mathrm{SU}(2)_L$ scalar singlet with hypercharge equal to zero, one can obtain another neutral Higgs boson that may mix with h. While for a charged Higgs boson the situation is different. Scalar singlet(s) with non-trivial hypercharge(s)[2] or higher multiplet(s) beyond the SM are needed. In the two-Higgs-doublet models (2HDMs) [8], there is one physical charged Higgs boson $H_D^{\pm}$ (the subscript "D" denotes doublet) in the particle spectrum. The couplings of $H_D^{\pm}$ to the fermions are proportional to fermion masses. It was noticed [9, 10] that in models with only Higgs doublets, there is no tree-level coupling of charged Higgs boson to $W^{\pm}$ and Z bosons. Although such interaction can be generated at loop level, it is usually suppressed [11–13]. Phenomenology of charged Higgs boson in the 2HDMs has been discussed thoroughly, see ref. [14] for a recent review.

If SM is extended with higher $\mathrm{SU}(2)_L$ representation of scalar field(s), the charged Higgs boson couples to $W^{\pm}Z$ at tree level. Models with $\mathrm{SU}(2)_L$ scalar triplet(s) are attractive since they can generate the neutrino mass [15–18] and provide dark matter candidate [19], etc. Nevertheless, in the models with one complex/real triplet, the $\rho = m_W^2/m_Z^2 \cos^2 \theta_W$ parameter deviates from unity, which constrains the triplet VEV

---

[1]We use the notation $Q = T_3 + Y$.

[2]Model-independent studies of singlet scalar with non-trivial hypercharge can be found in refs. [6, 7].

stringently. If one complex and one real triplets are introduced and the triplets have the same VEVs (In our convention, it corresponds to the case that the real triplet VEV is $1/\sqrt{2}$ of the complex triplet VEV, see more details in section 3), the relation $\rho = 1$ can be maintained at tree level [20]. This is protected by $\mathrm{SU}(2)_L \times \mathrm{SU}(2)_R \to \mathrm{SU}(2)_C$ of the Higgs potential surviving after the EWSB [21] similar with the SM. Here $\mathrm{SU}(2)_C$ represents the custodial symmetry [22]. An example of this type is Georgi-Machacek (GM) model, in which the triplet VEV can be large. There are two singly charged Higgs bosons $H_3^\pm$ and $H_5^\pm$ in the GM model, which transform as 3-plet and 5-plet under $\mathrm{SU}(2)_C$, respectively [21]. Due to the custodial symmetry, $H_3^\pm$ and $H_5^\pm$ couple to fermions and $W^\mp Z$ separately and there is no mixing between them. Besides, both the couplings of $H_3^\pm$ to fermions and $H_5^\pm$ to $W^\mp Z$ are proportional to the triplet VEV [23, 24].

Experimental searches for singly charged Higgs bosons have been carried out at high-energy colliders. The search strategies depend on the couplings of charged Higgs boson to SM particles. The LEP experiments have excluded the charged Higgs boson in the type-II 2HDM with mass below $80\,\mathrm{GeV}$ [25]. At the LHC, the $H_D^\pm$ in the 2HDMs is primarily produced from top quark decay when lighter than top quark, i.e. $m_{H_D^+} < m_t$ or in the association production with top quark if $m_{H_D^+} > m_t$. Various decay channels including[3] tb [26–28] $\tau\nu$ [28–31], cs [32] and cb [33] have been explored for $H_D^\pm$ in the mass range from $90\,\mathrm{GeV}$ to $2\,\mathrm{TeV}$ with no significant excess observed. For the $H_5^\pm$ in the GM model, it has been sought in the vector-boson-fusion (VBF) process $pp \to jjH_5^\pm$, $H_5^\pm \to W^\pm Z$ [34, 35] at the LHC for $200\,\mathrm{GeV} \leq m_{H_5^\pm} \leq 1\,\mathrm{TeV}$.

However, an interesting scenario in which $H^\pm$ couples to both fermions and $W^\mp Z$ significantly has not been extensively explored. Such a charged Higgs boson does not exist in many popular Higgs extended models, such as 2HDMs and GM model. Nevertheless, once a singly charged Higgs boson was discovered in one existing channel, its couplings to all SM particles are requested to verify its nature. In this scenario, new production and decay channels can be utilized. Since the couplings of $H^\pm$ to fermions are usually proportional to the fermion masses, its couplings to the third generation quarks are more relevant. The property of charged Higgs boson with both couplings to fermions and $W^\mp Z$ can be revealed through the processes: (1) $pp \to jjH^\pm$, $H^\pm \to tb$; (2) $pp \to tH^\pm$, $H^\pm \to W^\pm Z$. In this work, we will study the first process $pp \to jjH^\pm$, $H^\pm \to tb$ by investigating the sensitivity to the effective couplings of $H^\pm$ to $W^\mp Z$ and tb and discussing the implications in a realistic modified GM model [36, 37][4] Whereas, we emphasize that our results are model-independent and can be applied to other models with such charged Higgs boson(s). The second process is left for a future work

This paper is arranged as follows. In section 2, the effective $H^\pm W^\mp Z$ and $H^\pm tb$ couplings and decay branching ratios are discussed. With the effective operators, we perform a model-independent collider study with the currently available constraints and the projected sensitivity in our proposed search $pp \to jjH^\pm$, $H^\pm \to tb$. In section 3, we discuss the search of a charged Higgs in the modified GM model and the implications on model parameters. Section 4 summarizes our results.

---

[3]For simplicity, the notation "$f_1 f_2$" denotes $f_1 \bar{f}_2$ and $\bar{f}_1 f_2$, where $f_1 f_2 = tb, \tau\nu, cs, cb$.

[4]For studies on neutral Higgs couplings to gauge bosons in the modified GM model, see refs. [38, 39].

2 $H^\pm W^\mp Z$ and $H^\pm tb$ couplings and collider search strategies

The most general effective Lagrangian that describes the interactions of $H^\pm$ with $W^\pm Z$ and tb is parameterized as [40, 41]

$$\mathcal{L}_{\text{eff}} = g m_W F_{WZ} H^+ W_\mu^- Z^\mu - \sqrt{2}/v H^+ \bar{t}(m_t A_t P_L + m_b A_b P_R) b + h.c., \qquad (2.1)$$

where $P_{L/R} = (1 \mp \gamma_5)/2$, and $v \simeq 246\,\text{GeV}$. For $m_{H^+} > m_t + m_b$, the partial widths of H^+ into $W^+ Z$ and $t\bar{b}$ are given by

$$\Gamma(H^+ \to W^+ Z) = \frac{m_{H^+}}{16\pi} \lambda^{1/2}(1, x_W, x_Z) g^2 |F_{WZ}|^2 \left[\frac{(1 - x_W - x_Z)^2}{4 x_Z} + 2 x_W \right],$$

$$\Gamma(H^+ \to t\bar{b}) = \frac{3 g^2 |A_t|^2 m_t^2}{32\pi m_{H^+} m_W^2} (m_{H^+}^2 - m_t^2 - m_b^2) \lambda^{1/2}(1, x_t, x_b). \qquad (2.2)$$

Here g is $SU(2)_L$ gauge coupling, $\lambda(x, y, z) = (x - y - z)^2 - 4yz$ and $x_{W,Z,t,b} = m_{W,Z,t,b}^2/m_{H^+}^2$. The H^+ has the total width

$$\Gamma_{H^+} = \Gamma(H^+ \to W^+ Z) + \Gamma(H^+ \to t\bar{b}) + \Gamma(H^+ \to \text{others}), \qquad (2.3)$$

where $\Gamma(H^+ \to \text{others})$ denotes the partial width of H^+ into other final states. Since the couplings of H^+ to fermions are proportional to the fermion masses, the decay widths of H^+ into other fermions are much smaller. Thus it is plausible to assume that the total width of H^+ is saturated by decays into $W^+ Z$ and $t\bar{b}$ (minimal total width assumption). Decay branching ratios of $H^\pm \to t\bar{b}$ and $H^\pm \to W^\pm Z$ are expressed as

$$\mathcal{B}_{tb} \equiv \mathcal{B}(H^\pm \to tb) = \frac{\Gamma(H^+ \to t\bar{b})}{\Gamma(H^+ \to t\bar{b}) + \Gamma(H^+ \to W^+ Z)}, \qquad (2.4)$$

$$\mathcal{B}_{WZ} \equiv \mathcal{B}(H^\pm \to W^\pm Z) = \frac{\Gamma(H^+ \to W^+ Z)}{\Gamma(H^+ \to t\bar{b}) + \Gamma(H^+ \to W^+ Z)}. \qquad (2.5)$$

In the following, the effective couplings in eq. (2.1) will be adopted. We perform a model-independent analysis of the $pp \to jjH^\pm$, $H^\pm \to tb$ with leptonic decay of top quarks at the 13 TeV LHC. The charged Higgs boson mass is assumed to be in the range from 200 GeV to 1 TeV.[5] We note that in ref. [42], the process $pp \to jjH^\pm$, $H^\pm \to tb$ was also studied at the LHC. Only the effective coupling $H^\pm W^\mp Z$ was discussed, whereas how $H^\pm$ can simultaneously decay into tb was not explained [42]. We will perform a more detailed collider analysis in this section and investigate a realistic model, which has both tree-level couplings of $H^\pm W^\mp Z$ and $H^\pm tb$ in section 3.

We generate the signal and backgrounds $t\bar{t}$, tW and tq processes with $q = j, b$, using MG5_aMC@NLO v2.4.3 [43] at the parton level with following cuts to isolate objects:

$$p_T^{j,b} > 20\,\text{GeV}, p_T^\ell > 10\,\text{GeV}, \ \Delta R_{mn} > 0.2, \ |\eta_{j,b}| < 5, \ |\eta_{e,\mu}| < 2.5. \qquad (2.6)$$

In the above, $m, n = j, b, \ell$, j denotes light-flavor quarks, $\ell = e, \mu$, and the angular distance in the $\eta - \phi$ plane is defined as $\Delta R_{ij} \equiv \sqrt{(\eta_i - \eta_j)^2 + (\phi_i - \phi_j)^2}$ with η_i and ϕ_i being

---

[5]We choose this mass range to match the current searches in the VBF channels in refs. [34, 35].

the pseudo-rapidity and azimuthal angle of particle i, respectively. The NN23LO1 Parton Distribution Function (PDF) set [44] and default hadronization and factorization scales are used. The parton-level events are interfaced to `Pythia 6.4` [45] and `Delphes3 v3.3.3` [46] for parton shower and detector simulation. The backgrounds $t\bar{t}$, tW, tq are matched in 5-flavor scheme up to 1, 1 and 2 jets, respectively. Jets are clustered via the anti-k_t algorithm [47] with a radius parameter of $R = 0.4$ as implemented in `Fastjet` [48].

To select the signal process, we impose a series of selection cuts, which are composed of basic, VBF and optimal cuts. The *basic cuts* are used to identify objects at the hadron level:

(B-1) The angular separation is chosen as $\Delta R_{mn} > 0.4$, $m, n = j, b, \ell$.

(B-2) At least four jets with $p_T > 25\,\text{GeV}$ are tagged, and two or more of them are b-tagged. It is assumed that the b-tagging efficiency is 0.7, while the c quark and light flavor quark misidentification probability are 0.2 and 0.01, respectively [27, 49].

(B-3) Events with exactly one charged lepton with $p_T > 30\,\text{GeV}$ and no other charged lepton with $p_T > 10\,\text{GeV}$ are selected.

(B-4) It is required that the missing energy $E_T^{\text{miss}} > 30\,\text{GeV}$ [50] since there is a neutrino of the signal process in the final state.

The *VBF cuts* are adopted similar with those in refs. [34, 35]:

(V-1) There are at least two non-b-tagged jets in opposite detector hemispheres.

(V-2) The invariant mass and rapidity separation of the leading p_T jets in opposite hemispheres are used as $m_{jj} > 400\,\text{GeV}$, $|\Delta\eta_{jj}| > 3.5$.

High-p_T b-jets and charged lepton from the decay $H^{\pm} \to tb$, $t \to b\ell\nu$ can be further used to trigger the signal. Besides, since there is only one neutrino in the signal process, it is possible to fully reconstruct the four-momentum of top quark and the invariant mass of the charged Higgs boson $H^{\pm}$'s decay products. Depending on the kinematic distributions of p_T^{ℓ}, p_T^{b1}, p_T^{b2} and m_{tb} after the VBF cuts for each $m_{H^{\pm}}$ (see figure 1 for distributions with $m_{H^{\pm}} = 500\,\text{GeV}$), one can impose the *optimal cuts* as follows:

(O-1) The transverse momentum of charged lepton is larger than a minimum, $p_T^{\ell} > p_{T\min}^{\ell}$.

(O-2) Lower bounds or upper bounds of the transverse momenta of tagged b-jets are imposed depending on $m_{H^{\pm}}$,

- $p_T^{b1} < p_{T\max}^{b1}$, $p_T^{b2} < p_{T\max}^{b2}$ for $m_{H^{\pm}} \leq 225\,\text{GeV}$,
- $p_T^{b1} > p_{T\min}^{b1}$, $p_T^{b2} > p_{T\min}^{b2}$ for $m_{H^{\pm}} \geq 325\,\text{GeV}$,

where p_T^{b1} and p_T^{b2} denote the leading and sub-leading transverse momenta of b-jets.

(O-3) The four-momentum of top quark can be reconstructed using the template χ^2 method. For each event, the χ^2 is defined as [51]

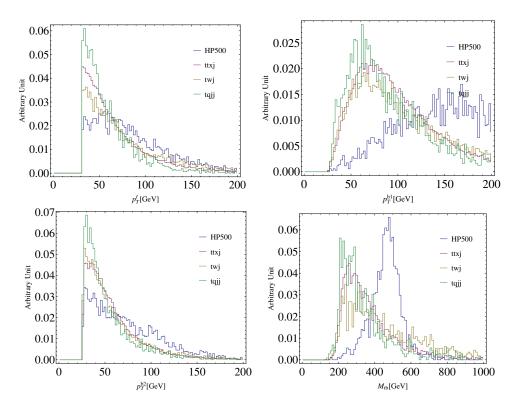$$\chi^2 = \left(\frac{m_{b\ell\nu} - m_t}{\Gamma_t}\right)^2,\tag{2.7}$$

Figure 1. Kinematic distributions of p_T^ℓ, p_T^{b1}, p_T^{b2} and m_{tb} after the VBF cuts for the charged Higgs boson mass $m_{H^\pm} = 500\,\text{GeV}$. Here "HP500" and "ttxj", "twj", "tqjj" denote the signal and backgrounds $t\bar{t}$, tW, tq, respectively.

where $m_t = 172.5\,\text{GeV}$ [52], $\Gamma_t = 4.08\,\text{GeV}$, $m_{b\ell\nu}$ denotes the invariant mass of lepton, neutrino and one b-jet. With the on-shell condition of W boson, we can determine the longitudinal transverse momentum of neutrino with a two-fold ambiguity [53]

$$p_L^\nu = \frac{1}{2(p_T^\ell)^2} \left[A_W p_L^\ell \pm E_\ell \sqrt{A_W^2 - 4(p_T^\ell)^2 (E_T^{\text{miss}})^2} \right], \tag{2.8}$$

where $A_W = m_W^2 + 2\vec{p}_T^{\,\ell} \cdot \vec{p}_T^{\,\text{miss}}$ and $m_W = 80.4\,\text{GeV}$. Furthermore, there are two b-jets in the final state.[6] By minimizing χ^2 [54], we can determine which b-jet originates from top quark decay and the sign of p_L^ν. Thus one is able to fully reconstruct the four-momentum of top quark and the invariant mass of t and b (m_{tb}). Since in the signal process, t and b come from the decay of on-shell charged Higgs boson $H^\pm$, the variable m_{tb} can be used to suppress the backgrounds. The cut on m_{tb} is optimized depending on $m_{H^\pm}$,

- $m_{tb}^{\text{min}} < m_{tb} < m_{tb}^{\text{max}}$.

---

[6]Actually, the additional b-jet may come from the parton-level scattering with initial b quark. However, such contribution should be small since the b-quark PDF is small. To reconstruct the top quark, we select the b-jet among the leading-p_T and sub-leading p_T b-jets.

$m_{H^\pm}$	$p^\ell_{T\mathrm{min}}$	$p^{b1}_{T\mathrm{min/max}}$	$p^{b2}_{T\mathrm{min/max}}$	m^{min}_{tb}	m^{max}_{tb}
200	−	70	40	−	250
225	−	75	50	−	250
250	−	−	−	−	300
275	−	−	−	−	350
300	−	−	−	−	350
325	−	70	−	250	350
350	−	80	−	250	400
375	−	90	−	275	450
400	−	100	−	300	500
450	−	110	60	350	550
500	50	120	65	400	600
550	70	130	65	450	650
600	75	140	70	450	700
700	75	150	75	500	800
800	85	160	75	500	1000
900	85	170	80	550	−
1000	90	170	80	600	−

Table 1. Bounds of kinematic variables in the mass range $200\,\mathrm{GeV} \leq m_{H^\pm} \leq 1000\,\mathrm{GeV}$. All numbers are in units of GeV. The symbol "−" indicates no cut being imposed.

Here, $p^\ell_{T\mathrm{min}}$ denotes the lower bound of p^ℓ_T. Similarly, $p^{b1}_{T\mathrm{min/max}}$, $p^{b2}_{T\mathrm{min/max}}$ and $m^{\mathrm{min/max}}_{tb}$ are the lower/upper bounds of p^{b1}_T, p^{b2}_T and m_{tb}, respectively. The explicit values are given in table 1.

After imposing the selection cuts, we find that the significance of the signal can be greatly improved. We show in table 2 the cut flow of the signal and background cross sections after each selection cut for $m_{H^\pm} = 500\,\mathrm{GeV}$ with the benchmark scenario $F_{WZ} = A_t = 0.5$. The discovery prospect and exclusion limit of the signal process are evaluated using [55]

$$\mathcal{Z}_D = \sqrt{2\left[(n_s + n_b)\log\frac{n_s + n_b}{n_b} - n_s\right]}, \tag{2.9}$$

$$\mathcal{Z}_E = \sqrt{-2\left[n_b\log\frac{n_s + n_b}{n_b} - n_s\right]}, \tag{2.10}$$

respectively. $n_s = \sigma_s\mathcal{L}$ and $n_b = \sigma_b\mathcal{L}$ denote the number of events after cuts with the integrated luminosity of $\mathcal{L}$, σ_s and σ_b are the cross sections of the signal and total background after cuts. The signal cross section σ_s can be expressed as

$$\begin{aligned}\sigma_s &= \sigma(pp \to jjH^\pm)\mathcal{B}(H^\pm \to tb)\epsilon_s, \\ &= \left[\sigma(pp \to jjH^\pm)_{\mathrm{BM}}\mathcal{B}(H^\pm \to tb)_{\mathrm{BM}}\epsilon_s\right]\frac{|F_{WZ}|^2}{0.5^2}\frac{\mathcal{B}(H^\pm \to tb)}{\mathcal{B}(H^\pm \to tb)_{\mathrm{BM}}},\end{aligned} \tag{2.11}$$
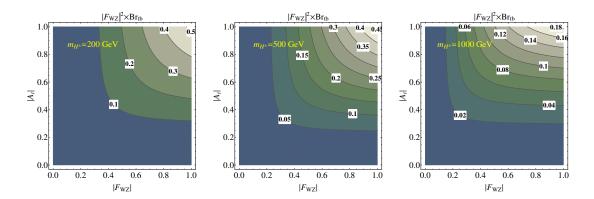
Figure 2. Dependence of $|F_{WZ}|^2 \times \mathcal{B}_{tb}$ on $|F_{WZ}|$ and $|A_t|$ for $m_{H^\pm} = 200, 500, 1000$ GeV.

cuts	signal	$t\bar{t}$	tW	tq
cuts in eq. (2.6)	7.76E-03	9.96E+01	1.04E+01	3.02E+01
$\Delta R_{mn} > 0.4$	7.76E-03	9.96E+01	1.04E+01	3.02E+01
$n_j \geq 4$	6.53E-03	8.06E+01	5.67E+00	4.16E+00
b-tagging	3.23E-03	3.14E+01	1.53E+00	1.28E+00
single lepton	2.03E-03	1.50E+01	7.97E-01	5.02E-01
$E_T^{\text{miss}} > 30$ GeV	1.62E-03	1.15E+01	6.12E-01	3.70E-01
≥ 2 non-b jets	1.35E-03	6.19E+00	3.12E-01	1.77E-01
$|\Delta \eta_{jj}| > 3.5$	1.02E-03	1.10E+00	5.35E-02	8.31E-02
$m_{jj} > 400$ GeV	9.52E-04	8.41E-01	3.94E-02	5.91E-02
$p_T^\ell > 50$ GeV	7.58E-04	5.10E-01	2.76E-02	2.92E-02
$p_T^{b1} > 120$ GeV, $p_T^{b2} > 65$ GeV	3.04E-04	9.13E-02	7.49E-03	4.78E-03
400 GeV $< m_{tb} < 600$ GeV	1.42E-04	2.33E-02	1.11E-03	7.88E-04

Table 2. The cut flow of the signal and background cross sections (in units of pb) for $m_{H^\pm} = 500$ GeV. The notation of "aE±0b" stands for $a \times 10^{\pm b}$.

where the quantities in the square bracket are obtained with the benchmark values $F_{WZ} = A_t = 0.5$. The signal cut efficiency ϵ_s is independent of the couplings F_{WZ} and A_t,[7] so that we are free to obtain it with the benchmark values of F_{WZ} and A_t. The signal cross section is proportional to $|F_{WZ}|^2 \times \mathcal{B}_{tb}$, which depends on $|F_{WZ}|$ and $|A_t|$ as shown in figure 2. We find that $|F_{WZ}|^2 \times \mathcal{B}_{tb}$ tends to be larger for a smaller $m_{H^\pm}$.

At the 13–14 TeV LHC, the integrated luminosity is planned to reach $3\,\text{ab}^{-1}$ [56]. In this work, we will study the process $pp \to jjH^\pm$, $H^\pm \to tb$ with integrated luminosity of $3\,\text{ab}^{-1}$ at the 13 TeV LHC. Using the relation in eqs. (2.9) (2.10) (2.11), we can obtain sensitivity to $|F_{WZ}|^2 \times \mathcal{B}(H^\pm \to tb)$ from the discovery prospects and exclusion limit of our proposed signal process $pp \to jjH^\pm$, $H^\pm \to tb$ as shown in figure 3. From this figure,

---

[7]We assume that the narrow width approximation is always valid for the signal process. For $|F_{WZ}|, |A_t| \lesssim 1$ and $m_{H^+} \leq 1000$ GeV, we obtain $\Gamma_{H^+}/m_{H^+} \lesssim 30\%$.
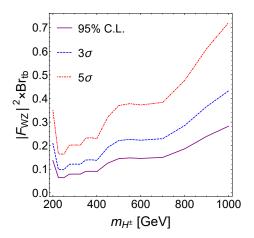
Figure 3. Sensitivities to $|F_{WZ}|^2 \times \mathcal{B}_{tb}$ in $pp \to jjH^{\pm}, H^{\pm} \to tb$ with the integrated luminosity of $3\,\mathrm{ab}^{-1}$.

one can find that, the scenarios with $|F_{WZ}|^2 \times \mathcal{B}(H^{\pm} \to tb) \gtrsim 0.43, 0.72$ can be observed at $3\sigma, 5\sigma$ for the charged Higgs boson in the mass range from $200\,\mathrm{GeV}$ to $1\,\mathrm{TeV}$, respectively. While the region of $|F_{WZ}|^2 \times \mathcal{B}(H^{\pm} \to tb) \gtrsim 0.25$ would be excluded at 95% confidence level (C.L.) or equivalently with $\mathcal{Z}_E \geq 1.96$. It is interesting to note that the sensitivity is the best for $m_{H^{\pm}} \simeq 250\,\mathrm{GeV}$ in the process $pp \to jjH^{\pm}, H^{\pm} \to tb$.

On the other hand, there are already experimental searches for charged Higgs bosons in the 2HDMs and the GM model. They provided constraints on $|A_t|^2 \times \mathcal{B}(H^{\pm} \to tb)$ and $|F_{WZ}|^2 \times \mathcal{B}(H^{\pm} \to W^{\pm}Z)$, respectively. To recast current constraints, we generate the leading-order (LO) processes $pp \to \bar{t}H^{\pm}$ and $pp \to jjH^{\pm}$ in 5-flavor scheme using MG5_aMC@NLO v2.4.3 with $F_{WZ} = A_t = 0.5$. We denote the exclusion limits at 95% C.L. in refs. [26–28, 34, 35] of $\sigma(pp \to tH^{\pm})\mathcal{B}(H^{\pm} \to tb)$ and $\sigma(pp \to jjH^{\pm})\mathcal{B}(H^{\pm} \to W^{\pm}Z)$ as $[\sigma\mathcal{B}]_{tb}^{\mathrm{limit}}$ and $[\sigma\mathcal{B}]_{WZ}^{\mathrm{limit}}$, respectively. The upper limits can then be re-interpreted as

$$|A_t|^2/0.5^2 \times \sigma(pp \to tH^{\pm})_{\mathrm{BM}}\mathcal{B}(H^{\pm} \to tb) \leq [\sigma\mathcal{B}]_{tb}^{\mathrm{limit}}, \qquad (2.12)$$

$$|F_{WZ}|^2/0.5^2 \times \sigma(pp \to jjH^{\pm})_{\mathrm{BM}}\mathcal{B}(H^{\pm} \to W^{\pm}Z) \leq [\sigma\mathcal{B}]_{WZ}^{\mathrm{limit}}, \qquad (2.13)$$

where $\sigma(pp \to tH^{\pm})_{\mathrm{BM}}$ and $\sigma(pp \to jjH^{\pm})_{\mathrm{BM}}$ denote the LO cross sections[8] of the $pp \to tH^{\pm}$ and the $pp \to jjH^{\pm}$, respectively. The constraints on $|F_{WZ}|^2 \times \mathcal{B}(H^{\pm} \to W^{\pm}Z)$ and $|A_t|^2 \times \mathcal{B}(H^{\pm} \to tb)$ are shown in figure 4. One can see that the constraints at the $13\,\mathrm{TeV}$ LHC are more stringent than those at the $8\,\mathrm{TeV}$ LHC, except for $300\,\mathrm{GeV} < m_{H^{\pm}} < 450\,\mathrm{GeV}$ in the process $pp \to jjH^{\pm}, H^{\pm} \to W^{\pm}Z$. In the following analysis, we take the strongest constraints in the range of $m_{H^{\pm}}$ from $200\,\mathrm{GeV}$ to $1\,\mathrm{TeV}$. On account of benchmark mass points in ref. [34], we will choose the mass interval of $100\,\mathrm{GeV}$ to illustrate the combined sensitivities in figure 5 and figure 7.

With the minimal total width assumption, we can express the branching ratios $\mathcal{B}(H^{\pm} \to tb)$ and $\mathcal{B}(H^{\pm} \to W^{\pm}Z)$ in terms of the effective couplings F_{WZ} and A_t. Therefore, we can obtain the discovery prospects and 95% C.L. exclusion limits in the plane of

---

[8]The next-to-leading-order cross sections of charged Higgs boson production in this channel are available but model-dependent, see refs. [57–59] and references therein.
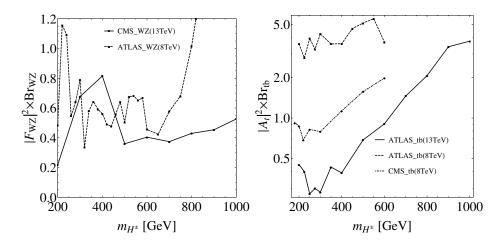
Figure 4. Constraints on $|F_{WZ}|^2 \times \mathcal{B}_{WZ}$ (left panel) and $|A_t|^2 \times \mathcal{B}_{tb}$ (right panel) from the existing charged Higgs boson searches at the LHC.

$|F_{WZ}|$ and $|A_t|$. In figure 5, scenarios outside of the shaded regions are excluded at 95% C.L. by the existing searches or our proposed search. The dashed and dot-dashed curves correspond to the discovery significance of 3σ, 5σ, respectively. For brevity, the processes $pp \to tH^{\pm}$, $H^{\pm} \to tb$ and $pp \to jjH^{\pm}$, $H^{\pm} \to W^{\pm}Z$ are denoted as tb and WZ modes, respectively. The process $pp \to jjH^{\pm}$, $H^{\pm} \to tb$ that depends on both the $H^{\pm}W^{\mp}Z$ and $H^{\pm}tb$ couplings is denoted as the mixed mode. We find that for $300\,\mathrm{GeV} \lesssim m_{H^{\pm}} \lesssim 400\,\mathrm{GeV}$ with $|F_{WZ}|, |A_t| \sim 0.5$–1.0, $H^{\pm}$ that couples to $W^{\pm}Z$ and tb can be discovered in the process $pp \to jjH^{\pm}$, $H^{\pm} \to tb$ at $\mathcal{Z}_D \geq 5$. For lighter or heavier charged Higgs boson, we can still achieve regions of the effective couplings that correspond to $\mathcal{Z}_D \geq 3$. If $m_{H^{\pm}} \geq 500\,\mathrm{GeV}$, top quark from the decay of $H^{\pm}$ is boosted. It is possible to improve the significance with jet substructure techniques [27, 60], which is beyond the scope of this study. On the other hand, if a null result is observed, 95% C.L. exclusion limits in the plane of $|F_{WZ}|$ and $|A_t|$ are imposed. We obtain the most sensitive constraints on models with both $H^{\pm}W^{\mp}Z$ and $H^{\pm}tb$ couplings from the process $pp \to jjH^{\pm}$, $H^{\pm} \to tb$ for $|F_{WZ}|, |A_t| \sim 1.0$.

3 Modified GM model with both $H^{\pm}W^{\mp}Z$ and $H^{\pm}tb$ couplings

In this section, we will investigate a realistic model with nonvanishing $H^{\pm}W^{\mp}Z$ and $H^{\pm}tb$ couplings. Recall that in the GM model [20, 21], there are two singly charged Higgs boson $H_3^{\pm}$ and $H_5^{\pm}$, which interact with fermions and $W^{\mp}Z$ separately since they transform in different custodial symmetry $\mathrm{SU}(2)_C$ representations. It was found [36, 61] that if the custodial symmetry in the Higgs potential is relaxed, these two charged Higgs bosons can in general mix with each, resulting in two mass eigenstates that couple to both $W^{\pm}Z$ and tb. We will refer this model as the modified GM model. However, we emphasize that it is just a representative model. For example, in a supersymmetric model [62, 63], charged Higgs bosons can also couple to $W^{\pm}Z$ and fermions simultaneously due to the custodial symmetry breaking and doublet-triplet mixing. Our results in section 2 can be applied
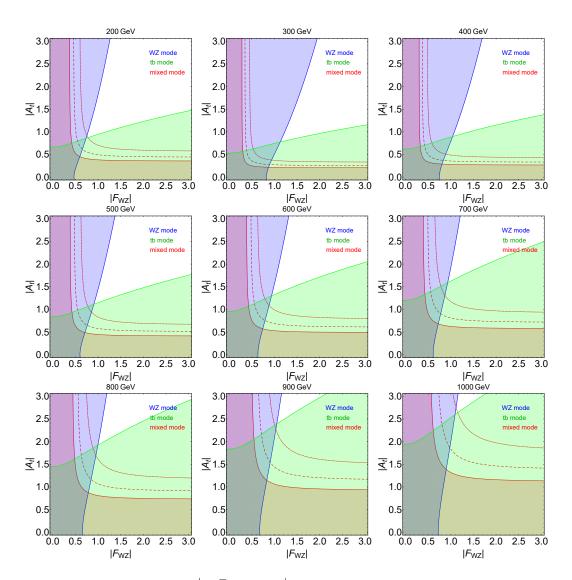
Figure 5. Sensitivities to the $H^{\pm}W^{\mp}Z$ and $H^{\pm}tb$ couplings for $m_{H^{\pm}} = 200$–$1000\,\mathrm{GeV}$ with the minimal total width assumption. The blue and green regions are obtained from the exclusion limits at 95% C.L. of the processes $pp \to tH^{\pm}$, $H^{\pm} \to tb$ and $pp \to jjH^{\pm}$, $H^{\pm} \to W^{\pm}Z$, respectively. The red solid, dashed and dot-dashed curves correspond to the exclusion limits at 95% C.L. and discovery significance $\mathcal{Z}_D = 3, 5$, respectively.

to any model with $H^{\pm}W^{\mp}Z$ and $H^{\pm}tb$ interactions. Below we will briefly introduce the modified GM model and show the implications in terms of the model parameters.

As in the original GM model [20, 21], we introduce two Higgs triplets: one real triplet $\xi \sim (3,0)$ and one complex triplet $\chi \sim (3,1)$, which have the following forms:

$$\chi = \begin{pmatrix} \chi^{+}/\sqrt{2} & \chi^{++} \\ \chi^{0} & -\chi^{+}/\sqrt{2} \end{pmatrix}, \quad \xi = \begin{pmatrix} \xi^{0}/\sqrt{2} & \xi^{+} \\ \xi^{-} & -\xi^{0}/\sqrt{2} \end{pmatrix} \tag{3.1}$$

with the conventions $\xi^{-} = (\xi^{+})^{*}$, $\chi^{0} = (v_{\chi} + h_{\chi} + iI_{\chi})/\sqrt{2}$ and $\xi^{0} = v_{\xi} + h_{\xi}$.

In order to discuss mass eigenstates of charged Higgs fields, it is convenient to use the basis (G^+, H_3^+, H_5^+),

$$\begin{pmatrix} G^+ \\ H_3^+ \\ H_5^+ \end{pmatrix} = \begin{pmatrix} \dfrac{v_H}{v} & \dfrac{2v_\xi}{v} & -\dfrac{\sqrt{2}v_\chi}{v} \\ -\dfrac{4v_\xi^2 + 2v_\chi^2}{N_2} & \dfrac{2v_H v_\xi}{N_2} & -\dfrac{\sqrt{2}v_H v_\chi}{N_2} \\ 0 & \dfrac{\sqrt{2}v_\chi}{N_3} & \dfrac{2v_\xi}{N_3} \end{pmatrix} \begin{pmatrix} h^+ \\ \xi^+ \\ \chi^+ \end{pmatrix}, \qquad (3.2)$$

where $v \equiv \sqrt{v_H^2 + 4v_\xi^2 + 2v_\chi^2} \simeq 246\,\text{GeV}$ and the constants N_i are given by $N_2 = \sqrt{(4v_\xi^2 + 2v_\chi^2)^2 + 4v_H^2 v_\xi^2 + 2v_H^2 v_\chi^2}$ and $N_3 = \sqrt{2v_\chi^2 + 4v_\xi^2}$. The Goldstone mode G^+ is "eaten" by W^+, while H_3^+ and H_5^+ are not mass eigenstates in general unless there is custodial symmetry in the Higgs potential. One needs to further diagonalize the mass matrix to obtain the mass eigenstates H_3^{m+} and H_5^{m+},

$$\begin{pmatrix} H_3^+ \\ H_5^+ \end{pmatrix} = \begin{pmatrix} \cos\delta & \sin\delta \\ -\sin\delta & \cos\delta \end{pmatrix} \begin{pmatrix} H_3^{m+} \\ H_5^{m+} \end{pmatrix}. \qquad (3.3)$$

The explicit form of the mixing angle δ can be found in ref. [36].

The interactions of $H_3^{m\pm}$, $H_5^{m\pm}$ with $W^\mp Z$ and quarks are

$$\mathcal{L}_{W^\pm Z} = \left(\frac{g^2}{2c_W} \frac{v_H(2v_\chi^2 - 4v_\xi^2)}{N_2} \cos\delta + \frac{g^2}{2c_W} \frac{4\sqrt{2}v_\chi v_\xi}{N_3} \sin\delta \right) H_3^{m+} W_\mu^- Z^\mu$$

$$+ \left(\frac{g^2}{2c_W} \frac{v_H(2v_\chi^2 - 4v_\xi^2)}{N_2} \sin\delta - \frac{g^2}{2c_W} \frac{4\sqrt{2}v_\chi v_\xi}{N_3} \cos\delta \right) H_5^{m+} W_\mu^- Z^\mu + h.c., \quad (3.4)$$

$$\mathcal{L}_{\text{Yuk}}^q = -\sqrt{2}\frac{1}{v_H} \frac{4v_\xi^2 + 2v_\chi^2}{N_2} \left(\bar{U}\hat{M}_u V_{\text{CKM}} P_L D - \bar{U} V_{\text{CKM}} \hat{M}_d P_R D \right)$$

$$\times \left(\cos\delta H_3^{m+} + \sin\delta H_5^{m+} \right) + h.c.,$$

where $c_W \equiv \cos\theta_W$, $U = (u, c, t)^T$, $D = (d, s, b)^T$ and V_{CKM} denotes the Cabibbo-Kobayashi-Maskawa matrix. The ρ parameter is expressed as

$$\rho = \frac{v_H^2 + 2v_\chi^2 + 4v_\xi^2}{v_H^2 + 4v_\chi^2}. \qquad (3.5)$$

With custodial symmetry, $v_\xi = v_\chi/\sqrt{2}$ and $\sin\delta = 0$, thus $\rho = 1$ and $H_5^{m\pm}(= H_5^\pm)$ does not couple to quarks, whereas $H_3^{m\pm}(= H_3^\pm)$ does not couple to $W^\mp Z$ at tree level.

Since the ρ parameter is severely constrained, $\rho^{\text{exp}} = 1.00039 \pm 0.00017$ [52], the v_χ, v_ξ are generally constrained to be less than a few GeV if they are independent. However when $v_\xi = v_\chi/\sqrt{2}$, one has $\rho = 1$, and larger v_χ and v_ξ are allowed. In this case, $\tan 2\delta$ is proportional to the combination $2v_\chi(-\sqrt{2}\mu_{\chi HH} + \mu_{\xi HH}) + v_\chi^2(\kappa_3 + \sqrt{2}\lambda)$, where $\mu_{\chi HH}$, $\mu_{\xi HH}$, κ_3 and λ are the couplings in the general Higgs potential [36].[9] In the GM model

---

[9]If the custodial symmetry is removed, these couplings are independent, while in the GM model, $\mu_{\xi HH} = \sqrt{2}\mu_{\chi HH}$ and $\kappa_3 = -\sqrt{2}\lambda_5$ [36].

this combination is forced to be zero by the custodial symmetry. However, if the custodial symmetry is broken explicitly the mixing angle δ can be sizable. We will work in the modified GM (MGM) model with the working hypothesis $v_\xi = v_\chi/\sqrt{2}$.

The interactions of charged Higgs bosons to quarks and $W^\pm Z$ in the MGM model can be expressed as

$$\mathcal{L}_{W^\pm Z} = \frac{g^2 v_\chi}{c_W} W_\mu^- Z^\mu (\sin\delta H_3^{m+} - \cos\delta H_5^{m+}) + h.c., \tag{3.6}$$

$$\mathcal{L}_{\text{Yuk}}^q = -\frac{2\sqrt{2} v_\chi}{v_H v}(\bar{U}\hat{M}_u V_{\text{CKM}} P_L D - \bar{U} V_{\text{CKM}} \hat{M}_d P_R D)(\cos\delta H_3^{m+} + \sin\delta H_5^{m+}) + h.c., \tag{3.7}$$

where

$$N_2 = 2v_\chi v, \quad N_3 = 2v_\chi, \quad v = \sqrt{v_H^2 + 4v_\chi^2}. \tag{3.8}$$

The mixing angle δ is in the range of $[0, 2\pi)$, so $H_3^{m\pm}$ and $H_5^{m\pm}$ can interact with both quarks and $W^\pm Z$ unless $\delta = n\pi/2$ with $n = 0, 1, 2, 3$.

Compared with the Lagrangian in eq. (2.1), we can obtain the effective couplings F_{WZ}, A_t and A_b as follows:

$$F_{WZ} = \frac{g v_\chi}{c_W m_W}\sin\delta, \quad A_t = -A_b = \frac{2v_\chi}{v_H}V_{tb}\cos\delta, \tag{3.9}$$

for the $H_3^{m\pm}$ and

$$F_{WZ} = -\frac{g v_\chi}{c_W m_W}\cos\delta, \quad A_t = -A_b = \frac{2v_\chi}{v_H}V_{tb}\sin\delta, \tag{3.10}$$

for the $H_5^{m\pm}$. Combined with the effective Lagrangian in eq. (2.1), it is apparent that the magnitudes of the right-handed $H^\pm tb$ couplings are suppressed and smaller than the left-handed one by a factor of m_b/m_t.

The couplings of $H_3^{m\pm}$ and $H_5^{m\pm}$ to quarks and $W^\mp Z$ are proportional to the triplet VEV v_χ, which is a generic feature of the GM-type models [64]. A larger triplet VEV can result in a better sensitivity. With the sum rule $v_H^2 + 4v_\chi^2 = v^2$ in the MGM model, the triplet VEV $v_\chi = \sqrt{v^2 - v_H^2}/2 \lesssim 88, 121, 123\,\text{GeV}$ is required in order to satisfy the perturbative bound of the top Yukawa coupling $m_t/v_H \lesssim 1, \sqrt{4\pi}, 4\pi$ from the renormalization group running [65, 66]. Moreover, in general we can obtain a strict upper bound on the triplet VEV from the perturbative unitarity of the scattering amplitude for $t\bar{t} \to t\bar{t}$ [67, 68]. One can obtain that $y_t \lesssim \sqrt{16\pi/5}$, which implies that the doublet VEV $v_H \gtrsim 78\,\text{GeV}$. In the MGM model, the couplings of the neutral Higgs bosons to $t\bar{t}$ also depend on other parameters compared with the model discussed in refs. [67, 68]. But the constrain can still provide some guide for the allowed Yukawa coupling, so that the triplet VEV $v_\chi \lesssim 117\,\text{GeV}$.

On the other hand, the $H_3^{m\pm}tb$ and $H_5^{m\pm}tb$ couplings can also modify the $Zb\bar{b}$ coupling through higher order corrections. At the 1-loop level, the correction to the left-handed

coupling is expressed as [61, 69]

$$
\begin{aligned}
\delta g_{\mathrm{MGM}}^{L} = {} & \frac{1}{32\pi^2}\frac{e}{s_W c_W}\left(\frac{gm_t}{\sqrt{2}m_W}\right)^2 \tan^2\theta_H \Bigg\{ \sin^2\delta\left[\frac{R_5}{R_5-1} - \frac{R_5\log R_5}{(R_5-1)^2}\right] \\
& + \cos^2\delta\left[\frac{R_3}{R_3-1} - \frac{R_3\log R_3}{(R_3-1)^2}\right]\Bigg\} + \frac{1}{16\pi^2}\frac{e}{s_W c_W}\left(\frac{gm_t}{\sqrt{2}m_W}\right)^2 \tan^2\theta_H \\
& \times (2\cos\theta_H\sin\delta\cos\delta)\Bigg\{ C_{24}\left(m_t^2, m_W^2, m_{H_3^{m+}}^2\right) - C_{24}\left(m_t^2, m_W^2, m_{H_5^{m+}}^2\right) \\
& + \sin^2\delta\left[C_{24}\left(m_t^2, m_{H_5^{m+}}^2, m_{H_5^{m+}}^2\right) - C_{24}\left(m_t^2, m_{H_5^{m+}}^2, m_{H_3^{m+}}^2\right)\right] \\
& + \cos^2\delta\left[C_{24}\left(m_t^2, m_{H_5^{m+}}^2, m_{H_3^{m+}}^2\right) - C_{24}\left(m_t^2, m_{H_3^{m+}}^2, m_{H_3^{m+}}^2\right)\right] \Bigg\}, \quad (3.11)
\end{aligned}
$$

where $R_3 = m_t^2/m_{H_3^{m+}}^2$, $R_5 = m_t^2/m_{H_5^{m+}}^2$, $\tan\theta_H \equiv 2v_\chi/v_H$ and $\cos\theta_H \equiv v_H/v$. The first three arguments (m_b^2, m_Z^2, m_b^2) of the three-point integrals C_{24} [69] are dropped for simplicity. The first term is positive definite while the second term can be positive or negative. If $\sin\delta\cos\delta > 0$, the second term is negative for $m_{H_3^{m+}} > m_{H_5^{m+}}$ and cancels the contribution from the first term. On the other hand, the correction to the right-handed coupling $\delta g_{\mathrm{MGM}}^R$ is proportional to b-quark mass and negligible. The modifications of the $Zb\bar{b}$ coupling have been measured in the hadronic branching ratio $R_b \equiv \Gamma(Z \to b\bar{b})/\Gamma(Z \to \text{hadronic})$ [52],

$$
R_b^{\mathrm{exp}} = 0.21629 \pm 0.00066. \quad (3.12)
$$

The theoretical R_b in the MGM model is expressed as

$$
R_b^{\mathrm{MGM}} = R_b^{\mathrm{SM}} + \delta R_b^{\mathrm{MGM}}, \quad (3.13)
$$

where the SM value $R_b^{\mathrm{SM}} = 0.2158$ [52], $\delta R_b^{\mathrm{MGM}}$ that depends on $\delta g_{\mathrm{MGM}}^L$ can be parameterized as [61]

$$
\delta R_b^{\mathrm{MGM}} = -0.7785 \delta g_{\mathrm{MGM}}^L. \quad (3.14)
$$

Again, $\delta g_{\mathrm{MGM}}^R$ is neglected. Given the values of $m_{H_5^{m+}}$ and $m_{H_5^{m+}}$, R_b^{MGM} only depends on v_χ and $\sin\delta$. The 1σ and 2σ constraints from R_b measurements are implemented by requiring

$$
|R_b^{\mathrm{MGM}} - (R_b^{\mathrm{exp}})_{\mathrm{cent}}| < (R_b^{\mathrm{exp}})_{\mathrm{err}}, 2 \times (R_b^{\mathrm{exp}})_{\mathrm{err}}. \quad (3.15)
$$

Here the subscripts "cent" and "err" denote the central value and error of R_b^{exp} in eq. (3.12).

In figure 6, we show the $1\sigma, 2\sigma$ contours in the plane of v_χ and $\sin\delta$ for $m_{H_5^{m+}} = 200$, 500, 1000 GeV with the assumption $m_{H_3^{m+}} = 3m_{H_5^{m+}}$. We find that $v_\chi \lesssim 100$ GeV is still allowed by the $Zb\bar{b}$ data, while the exact upper limit depends on the mixing angle δ and the interplay of two charged Higgs bosons $H_3^{m\pm}$ and $H_5^{m\pm}$. Therefore, we do not show the $Zb\bar{b}$ constraint explicitly in the sensitivity plots in figure 7 and figure 8.
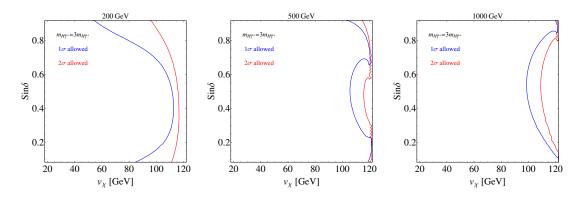
Figure 6. Constraints on the triplet VEV v_χ as well as sine of the mixing angle δ in the MGM model with the assumption $m_{H_3^{m+}} = 3 m_{H_5^{m+}}$. The mass of charged Higgs boson H_5^{m+} is chosen to be $200, 500, 1000 \, \text{GeV}$ from left to right panels. The region on the left of the blue (red) curve is allowed at 1σ (2σ) level.

In section 2, we have obtained the model-independent sensitivities to the effective $H^\pm W^\mp Z$ and $H^\pm tb$ couplings. Having the explicit forms of F_{WZ} and A_t in the MGM model in eqs. (3.9) (3.10), we can obtain the sensitivities to the model parameters. i.e., the mixing parameter δ and the triplet VEV v_χ. We assume that the charged Higgs boson $H^\pm$ is identified as $H_5^{m\pm}$, and it mainly decays into $W^\pm Z$ and tb. In the mass range from $200 \, \text{GeV}$ to $1 \, \text{TeV}$, sensitivities to v_χ and $|\sin \delta|$ are shown in figure 7. In accord with figure 5, the charged Higgs boson $H_5^{m\pm}$ can be discovered ($\mathcal{Z}_D \geq 5$) in the process $pp \to jj H^\pm$, $H^\pm \to tb$ for $300 \, \text{GeV} \lesssim m_{H_5^{m\pm}} \lesssim 400 \, \text{GeV}$ with the triplet VEV $80 \, \text{GeV} \lesssim v_\chi \lesssim 100 \, \text{GeV}$. On the other hand, if the $H_5^{m\pm}$ is not found, one can put 95% C.L. exclusion limits of the signal process in the plane of v_χ and $|\sin \delta|$. Especially, $v_\chi \lesssim 53, 62 \, \text{GeV}$ for $|\sin \delta| \simeq 0.7$ can be achieved with $m_{H_5^{m\pm}} = 300, 400 \, \text{GeV}$, which are well below the upper limits $90, 80 \, \text{GeV}$ for $|\sin \delta| = 0$, respectively. To evaluate the sensitivities to the triplet VEV as a function of the charged Higgs boson mass. We choose that $|\sin \delta| = 1/\sqrt{2}$, and obtain the sensitivities in the plane of $m_{H_5^{m\pm}}$ and v_χ in figure 8. The current constraint obtained from the exclusion limit in the process $pp \to t H^\pm$, $H^\pm \to tb$ is shown in the green curve, while there is no useful constraint from the process $pp \to jj H^\pm$, $H^\pm \to W^\pm Z$. The $3\sigma, 5\sigma$ discovery prospects and exclusion limit at 95% C.L. in the process $pp \to jj H^\pm$, $H^\pm \to tb$ are also shown. Both of the processes $pp \to jj H^\pm$, $H^\pm \to tb$ and $pp \to t H^\pm$, $H^\pm \to tb$ get the best sensitivities for $m_{H_5^{m\pm}} \simeq 250 \, \text{GeV}$ resulting dips in the curves. We obtain that the sensitivity to the triplet VEV v_χ of our proposed search is better than that of the existing searches. For the $m_{H_5^{m\pm}} \lesssim 500 \, \text{GeV}$, the region of the triplet VEV $v_\chi \lesssim 80 \, \text{GeV}$ can be probed at 95% C.L., shown as the purple curve in figure 8.

Before enclosing this section, we emphasize that the MGM model is only a representative model. Other models with triplets or higher $SU(2)_L$ representation of Higgs multiplets, in which charged Higgs boson(s) can couple to fermions and $W^\pm Z$ simultaneously, can be studied similarly.
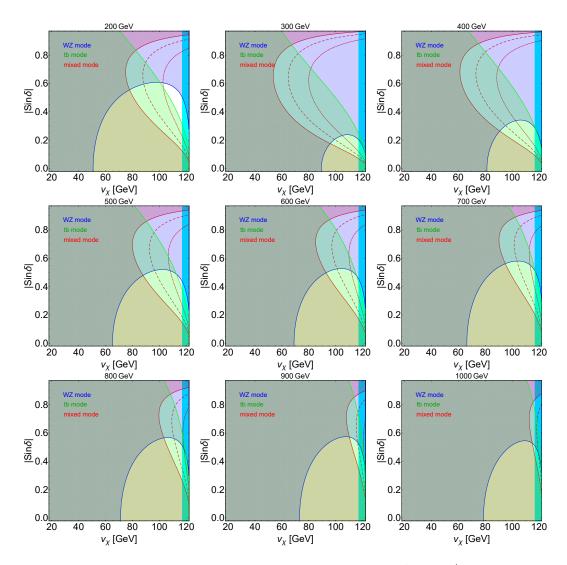
Figure 7. Sensitivities to v_χ and $|\sin\delta|$ in the MGM model with $H^\pm = H_5^{m\pm}$ for $m_{H_5^{m\pm}} = 200$–1000 GeV with the minimal total width assumption. The blue and green regions are obtained from the exclusion limit at 95% C.L. of the processes $pp \to tH^\pm$, $H^\pm \to tb$ and $pp \to jjH^\pm$, $H^\pm \to W^\pm Z$, respectively. The red solid, dashed and dot-dashed curves correspond to the exclusion limit at 95% C.L. and discovery prospects with $\mathcal{Z}_D = 3, 5$, respectively. The cyan vertical regions on the right of the panels are excluded by the perturbative unitarity requirement.

4 Conclusions

In this work, we have extended the existing searches of charged Higgs boson at the LHC. Different from the processes inspired by the 2HDMs and GM model, the VBF process $pp \to jjH^\pm$, $H^\pm \to tb$ requires the existence of both $H^\pm W^\mp Z$ and $H^\pm tb$ couplings. We have performed a model-independent analysis of this process at the LHC with the effective $H^\pm W^\mp Z$ and $H^\pm tb$ couplings. With the minimal total width assumption, we interpret the results in terms of the effective couplings F_{WZ} and A_t for $m_{H^\pm}$ in the range from 200 GeV to 1 TeV. We found that the process $pp \to jjH^\pm$, $H^\pm \to tb$ can be discovered ($\mathcal{Z}_D \geq 5$)

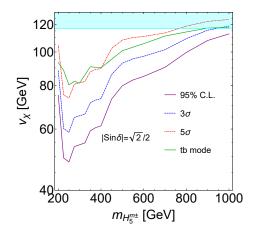**Figure 8**. Sensitivities to the $m_{H_5^{m\pm}}$ and v_χ in the MGM model in the mass range from $200\,\mathrm{GeV}$ to $1\,\mathrm{TeV}$ with the assumption $|\sin\delta| = 1/\sqrt{2}$. The cyan horizontal region is excluded by the perturbative unitarity requirement.

for $300\,\mathrm{GeV} \lesssim m_{H^\pm} \lesssim 400\,\mathrm{GeV}$ with $|F_{WZ}|, |A_t| \sim 0.5\text{–}1.0$. Discovering the process in the region of $m_{H^\pm} \geq 500\,\mathrm{GeV}$ requires the improved experimental selection criteria. However, one can still obtain the most sensitive constraints on models with both $H^\pm W^\mp Z$ and $H^\pm tb$ couplings through this process.

We investigate the implications in a realistic model, the MGM model, which introduces two Higgs triplets into the SM analogous to the GM model. Since the requirement of custodial symmetry in the Higgs potential after the EWSB is relaxed, two physical singly charged Higgs bosons $H_3^{m\pm}$ and $H_5^{m\pm}$ with both couplings to quarks and $W^\pm Z$ are achieved. We discuss the theoretical as well as experimental constraints of this model. Then the sensitivities to the model parameters, i.e., the triplet VEV v_χ and the mixing angle δ are obtained and compared with constraints from the existing searches if the charged Higgs boson $H^\pm$ is identified as $H_5^{m\pm}$. We have pointed out that $H_5^{m\pm}$ can be discovered in the process $pp \rightarrow jjH^\pm$, $H^\pm \rightarrow tb$ for $300\,\mathrm{GeV} \lesssim m_{H_5^{m\pm}} \lesssim 400\,\mathrm{GeV}$ with $80\,\mathrm{GeV} \lesssim v_\chi \lesssim 100\,\mathrm{GeV}$. Supposing a maximal mixing pattern with $|\sin\delta| = 1/\sqrt{2}$, the exclusion limit at 95% C.L. on the triplet VEV $v_\chi \lesssim 80\,\mathrm{GeV}$ can be achieved for $m_{H_5^{m\pm}} \lesssim 500\,\mathrm{GeV}$.

Finally, the signal process proposed in this work is a direct evidence for a charged Higgs boson that couples to fermions and $W^\pm Z$, which is complementary to current searches for charged Higgs bosons. Our study in this work can be used as a roadmap of future charged Higgs boson searches at the LHC.

Acknowledgments

References

[1] ATLAS collaboration, *Observation of a new particle in the search for the Standard Model Higgs boson with the ATLAS detector at the LHC*, *Phys. Lett.* **B 716** (2012) 1 [`arXiv:1207.7214`] [INSPIRE].

[2] CMS collaboration, *Observation of a new boson at a mass of 125 GeV with the CMS experiment at the LHC*, *Phys. Lett.* **B 716** (2012) 30 [`arXiv:1207.7235`] [INSPIRE].

[3] ATLAS and CMS collaborations, *Measurements of the Higgs boson production and decay rates and constraints on its couplings from a combined ATLAS and CMS analysis of the LHC pp collision data at $\sqrt{s} = 7$ and 8 TeV*, *JHEP* **08** (2016) 045 [`arXiv:1606.02266`] [INSPIRE].

[4] ATLAS collaboration, *Combined measurements of Higgs boson production and decay using up to 80 fb^{-1} of proton-proton collision data at $\sqrt{s} = 13$ TeV collected with the ATLAS experiment*, [ATLAS-CONF-2018-031](http://cds.cern.ch/record/2629412).

[5] CMS collaboration, *Combined measurements of the Higgs boson's couplings at $\sqrt{s} = 13$ TeV*, [CMS-PAS-HIG-17-031](http://cds.cern.ch/record/2308127).

[6] Q.-H. Cao, G. Li, K.-P. Xie and J. Zhang, *Searching for Weak Singlet Charged Scalar at the Large Hadron Collider*, *Phys. Rev.* **D 97** (2018) 115036 [`arXiv:1711.02113`] [INSPIRE].

[7] Q.-H. Cao, G. Li, K.-P. Xie and J. Zhang, *Searching for weak singlet charged scalar at lepton colliders*, `arXiv:1810.07659` [INSPIRE].

[8] G.C. Branco, P.M. Ferreira, L. Lavoura, M.N. Rebelo, M. Sher and J.P. Silva, *Theory and phenomenology of two-Higgs-doublet models*, *Phys. Rept.* **516** (2012) 1 [`arXiv:1106.0034`] [INSPIRE].

[9] J.A. Grifols and A. Mendez, *The $WZH^{\pm}$ Coupling in* SU(2) × U(1) *Gauge Models*, *Phys. Rev.* **D 22** (1980) 1725 [INSPIRE].

[10] J.F. Gunion, H.E. Haber, G.L. Kane and S. Dawson, *The Higgs Hunter's Guide*, *Front. Phys.* **80** (2000) 1 [INSPIRE].

[11] S. Kanemura, *Possible enhancement of the $e^+ e^- \to H^{\pm} W^{\mp}$ cross-section in the two Higgs doublet model*, *Eur. Phys. J.* **C 17** (2000) 473 [`hep-ph/9911541`] [INSPIRE].

[12] S. Moretti, D. Rojas and K. Yagyu, *Enhancement of the $H^{\pm} W^{\mp} Z$ vertex in the three scalar doublet model*, *JHEP* **08** (2015) 116 [`arXiv:1504.06432`] [INSPIRE].

[13] G. Abbas, D. Das and M. Patra, *Loop induced $H^{\pm} \to W^{\pm} Z$ decays in the aligned two-Higgs-doublet model*, *Phys. Rev.* **D 98** (2018) 115013 [`arXiv:1806.11035`] [INSPIRE].

[14] A.G. Akeroyd et al., *Prospects for charged Higgs searches at the LHC*, *Eur. Phys. J.* **C 77** (2017) 276 [`arXiv:1607.01320`] [INSPIRE].

[15] G. Lazarides, Q. Shafi and C. Wetterich, *Proton Lifetime and Fermion Masses in an* SO(10) *Model*, *Nucl. Phys.* **B 181** (1981) 287 [INSPIRE].

[16] M. Magg and C. Wetterich, *Neutrino Mass Problem and Gauge Hierarchy*, *Phys. Lett.* **B 94** (1980) 61 [INSPIRE].

[17] R.N. Mohapatra and G. Senjanović, *Neutrino Masses and Mixings in Gauge Models with Spontaneous Parity Violation*, *Phys. Rev.* **D 23** (1981) 165 [INSPIRE].

[18] T.P. Cheng and L.-F. Li, *Neutrino Masses, Mixings and Oscillations in* $\mathrm{SU}(2) \times \mathrm{U}(1)$ *Models of Electroweak Interactions*, *Phys. Rev.* **D 22** (1980) 2860 [INSPIRE].

[19] M. Cirelli, N. Fornengo and A. Strumia, *Minimal dark matter*, *Nucl. Phys.* **B 753** (2006) 178 [hep-ph/0512090] [INSPIRE].

[20] H. Georgi and M. Machacek, *Doubly charged Higgs bosons*, *Nucl. Phys.* **B 262** (1985) 463 [INSPIRE].

[21] M.S. Chanowitz and M. Golden, *Higgs Boson Triplets With* $M_W = M_Z \cos\theta_W$, *Phys. Lett.* **B 165** (1985) 105 [INSPIRE].

[22] P. Sikivie, L. Susskind, M.B. Voloshin and V.I. Zakharov, *Isospin Breaking in Technicolor Models*, *Nucl. Phys.* **B 173** (1980) 189 [INSPIRE].

[23] C.-W. Chiang and K. Yagyu, *Testing the custodial symmetry in the Higgs sector of the Georgi-Machacek model*, *JHEP* **01** (2013) 026 [arXiv:1211.2658] [INSPIRE].

[24] K. Hartling, K. Kumar and H.E. Logan, *The decoupling limit in the Georgi-Machacek model*, *Phys. Rev.* **D 90** (2014) 015007 [arXiv:1404.2640] [INSPIRE].

[25] ALEPH, DELPHI, L3, OPAL and LEP collaborations, *Search for Charged Higgs bosons: Combined Results Using LEP Data*, *Eur. Phys. J.* **C 73** (2013) 2463 [arXiv:1301.6065] [INSPIRE].

[26] ATLAS collaboration, *Search for charged Higgs bosons decaying into top and bottom quarks at* $\sqrt{s} = 13$ *TeV with the ATLAS detector*, *JHEP* **11** (2018) 085 [arXiv:1808.03599] [INSPIRE].

[27] ATLAS collaboration, *Search for charged Higgs bosons in the* $H^\pm \to tb$ *decay channel in pp collisions at* $\sqrt{s} = 8$ *TeV using the ATLAS detector*, *JHEP* **03** (2016) 127 [arXiv:1512.03704] [INSPIRE].

[28] CMS collaboration, *Search for a charged Higgs boson in pp collisions at* $\sqrt{s} = 8$ *TeV*, *JHEP* **11** (2015) 018 [arXiv:1508.07774] [INSPIRE].

[29] ATLAS collaboration, *Search for charged Higgs bosons decaying via* $H^\pm \to \tau^\pm\nu_\tau$ *in the* τ+*jets and* τ+*lepton final states with* $36\,fb^{-1}$ *of pp collision data recorded at* $\sqrt{s} = 13$ *TeV with the ATLAS experiment*, *JHEP* **09** (2018) 139 [arXiv:1807.07915] [INSPIRE].

[30] CMS collaboration, *Search for charged Higgs bosons with the* $H^\pm \to \tau^\pm\nu_\tau$ *decay channel in the fully hadronic final state at* $\sqrt{s} = 13$ *TeV*, CMS-PAS-HIG-16-031.

[31] ATLAS collaboration, *Search for charged Higgs bosons decaying via* $H^\pm \to \tau^\pm\nu$ *in fully hadronic final states using pp collision data at* $\sqrt{s} = 8$ *TeV with the ATLAS detector*, *JHEP* **03** (2015) 088 [arXiv:1412.6663] [INSPIRE].

[32] CMS collaboration, *Search for a light charged Higgs boson decaying to* $c\bar{s}$ *in pp collisions at* $\sqrt{s} = 8$ *TeV*, *JHEP* **12** (2015) 178 [arXiv:1510.04252] [INSPIRE].

[33] CMS collaboration, *Search for a charged Higgs boson decaying to charm and bottom quarks in proton-proton collisions at* $\sqrt{s} = 8$ *TeV*, *JHEP* **11** (2018) 115 [arXiv:1808.06575] [INSPIRE].

[34] CMS collaboration, *Search for Charged Higgs Bosons Produced via Vector Boson Fusion and Decaying into a Pair of W and Z Bosons Using pp Collisions at* $\sqrt{s} = 13$ *TeV*, *Phys. Rev. Lett.* **119** (2017) 141802 [arXiv:1705.02942] [INSPIRE].

[35] ATLAS collaboration, *Search for a Charged Higgs Boson Produced in the Vector-Boson Fusion Mode with Decay* $H^\pm \to W^\pm Z$ *using pp Collisions at* $\sqrt{s} = 8$ *TeV with the ATLAS Experiment*, *Phys. Rev. Lett.* **114** (2015) 231801 [arXiv:1503.04233] [INSPIRE].

[36] J.-Y. Cen, J.-H. Chen, X.-G. He and J.-Y. Su, *Impacts of multi-Higgs on the ρ parameter, decays of a neutral Higgs to WW and ZZ and a charged Higgs to WZ*, *Int. J. Mod. Phys.* **A 33** (2018) 1850152 [arXiv:1803.05254] [INSPIRE].

[37] S. Blasi, S. De Curtis and K. Yagyu, *Effects of custodial symmetry breaking in the Georgi-Machacek model at high energies*, *Phys. Rev.* **D 96** (2017) 015001 [arXiv:1704.08512] [INSPIRE].

[38] C.-W. Chiang, X.-G. He and G. Li, *Measuring the ratio of HWW and HZZ couplings through W^+W^-H production*, *JHEP* **08** (2018) 126 [arXiv:1805.01689] [INSPIRE].

[39] C.-W. Chiang and K. Yagyu, *Models with higher weak-isospin Higgs multiplets*, *Phys. Lett.* **B 786** (2018) 268 [arXiv:1808.10152] [INSPIRE].

[40] J.L. Diaz-Cruz, J. Hernandez-Sanchez and J.J. Toscano, *An Effective Lagrangian description of charged Higgs decays $H^+ \to W^+\gamma$, W^+Z and $W^+ h^0$*, *Phys. Lett.* **B 512** (2001) 339 [hep-ph/0106001] [INSPIRE].

[41] V.D. Barger, J.L. Hewett and R.J.N. Phillips, *New Constraints on the Charged Higgs Sector in Two Higgs Doublet Models*, *Phys. Rev.* **D 41** (1990) 3421 [INSPIRE].

[42] E. Asakawa, S. Kanemura and J. Kanzaki, *Potential for measuring the $H^\pm W^\mp Z_0$ vertex from WZ fusion at the Large Hadron Collider*, *Phys. Rev.* **D 75** (2007) 075022 [hep-ph/0612271] [INSPIRE].

[43] J. Alwall et al., *The automated computation of tree-level and next-to-leading order differential cross sections and their matching to parton shower simulations*, *JHEP* **07** (2014) 079 [arXiv:1405.0301] [INSPIRE].

[44] R.D. Ball et al., *Parton distributions with LHC data*, *Nucl. Phys.* **B 867** (2013) 244 [arXiv:1207.1303] [INSPIRE].

[45] T. Sjöstrand, S. Mrenna and P.Z. Skands, *PYTHIA 6.4 Physics and Manual*, *JHEP* **05** (2006) 026 [hep-ph/0603175] [INSPIRE].

[46] DELPHES 3 collaboration, *DELPHES 3, A modular framework for fast simulation of a generic collider experiment*, *JHEP* **02** (2014) 057 [arXiv:1307.6346] [INSPIRE].

[47] M. Cacciari, G.P. Salam and G. Soyez, *The anti-k_t jet clustering algorithm*, *JHEP* **04** (2008) 063 [arXiv:0802.1189] [INSPIRE].

[48] M. Cacciari, G.P. Salam and G. Soyez, *FastJet User Manual*, *Eur. Phys. J.* **C 72** (2012) 1896 [arXiv:1111.6097] [INSPIRE].

[49] CMS collaboration, *Identification of b quark jets at the CMS Experiment in the LHC Run 2*, CMS-PAS-BTV-15-001.

[50] ATLAS collaboration, *Search for vector-boson resonances decaying to a top quark and bottom quark in the lepton plus jets final state in pp collisions at $\sqrt{s} = 13\,TeV$ with the ATLAS detector*, *Phys. Lett.* **B 788** (2019) 347 [arXiv:1807.10473] [INSPIRE].

[51] A. Kobakhidze, L. Wu and J. Yue, *Anomalous Top-Higgs Couplings and Top Polarisation in Single Top and Higgs Associated Production at the LHC*, *JHEP* **10** (2014) 100 [arXiv:1406.1961] [INSPIRE].

[52] PARTICLE DATA GROUP collaboration, *Review of Particle Physics*, *Phys. Rev.* **D 98** (2018) 030001 [INSPIRE].

[53] E.L. Berger, Q.-H. Cao, J.-H. Yu and C.P. Yuan, *Calculation of Associated Production of a Top Quark and a W' at the LHC*, *Phys. Rev.* **D 84** (2011) 095026 [arXiv:1108.3613] [INSPIRE].

[54] ATLAS collaboration, *Search for $W' \to t\bar{b}$ in the lepton plus jets final state in proton-proton collisions at a centre-of-mass energy of $\sqrt{s} = 8\,TeV$ with the ATLAS detector*, *Phys. Lett.* **B 743** (2015) 235 [arXiv:1410.4103] [INSPIRE].

[55] G. Cowan, K. Cranmer, E. Gross and O. Vitells, *Asymptotic formulae for likelihood-based tests of new physics*, *Eur. Phys. J.* **C 71** (2011) 1554 [*Erratum ibid.* **C 73** (2013) 2501] [arXiv:1007.1727] [INSPIRE].

[56] G. Apollinari, O. Brüning, T. Nakamoto and L. Rossi, *High Luminosity Large Hadron Collider HL-LHC*, *CERN Yellow Report* (2015) 1 [arXiv:1705.08830] [INSPIRE].

[57] C. Degrande, M. Ubiali, M. Wiesemann and M. Zaro, *Heavy charged Higgs boson production at the LHC*, *JHEP* **10** (2015) 145 [arXiv:1507.02549] [INSPIRE].

[58] N. Kidonakis, *Theoretical results for charged-Higgs production*, in *13th Conference on the Intersections of Particle and Nuclear Physics (CIPANP 2018)*, Palm Springs, California, U.S.A., May 29–June 3, 2018 (2018) [arXiv:1808.02935] [INSPIRE].

[59] M. Zaro and H. Logan, *Recommendations for the interpretation of LHC searches for H_5^0, $H_5^\pm$, and $H_5^{\pm\pm}$ in vector boson fusion with decays to vector boson pairs*, LHCHXSWG-2015-001 [INSPIRE].

[60] ATLAS collaboration, *Search for $W' \to tb \to qqbb$ decays in pp collisions at $\sqrt{s} = 8\,TeV$ with the ATLAS detector*, *Eur. Phys. J.* **C 75** (2015) 165 [arXiv:1408.0886] [INSPIRE].

[61] H.E. Haber and H.E. Logan, *Radiative corrections to the $Zb\bar{b}$ vertex and constraints on extended Higgs sectors*, *Phys. Rev.* **D 62** (2000) 015011 [hep-ph/9909335] [INSPIRE].

[62] P. Bandyopadhyay, C. Corianò and A. Costantini, *General analysis of the charged Higgs sector of the $Y = 0$ triplet-singlet extension of the MSSM at the LHC*, *Phys. Rev.* **D 94** (2016) 055030 [arXiv:1512.08651] [INSPIRE].

[63] P. Bandyopadhyay and A. Costantini, *Distinguishing charged Higgs bosons from different representations at the LHC*, *JHEP* **01** (2018) 067 [arXiv:1710.03110] [INSPIRE].

[64] H.E. Logan and V. Rentala, *All the generalized Georgi-Machacek models*, *Phys. Rev.* **D 92** (2015) 075011 [arXiv:1502.01275] [INSPIRE].

[65] M.E. Machacek and M.T. Vaughn, *Two Loop Renormalization Group Equations in a General Quantum Field Theory. 2. Yukawa Couplings*, *Nucl. Phys.* **B 236** (1984) 221 [INSPIRE].

[66] W. Altmannshofer, M. Bauer and M. Carena, *Exotic Leptons: Higgs, Flavor and Collider Phenomenology*, *JHEP* **01** (2014) 060 [arXiv:1308.1987] [INSPIRE].

[67] M.S. Chanowitz, M.A. Furman and I. Hinchliffe, *Weak Interactions of Ultraheavy Fermions*, *Phys. Lett.* **B 78** (1978) 285 [INSPIRE].

[68] Z. Murdock, S. Nandi and Z. Tavartkiladze, *Perturbativity and a Fourth Generation in the MSSM*, *Phys. Lett.* **B 668** (2008) 303 [arXiv:0806.2064] [INSPIRE].

[69] H.E. Logan, *Radiative corrections to the $Zb\bar{b}$ vertex and constraints on extended Higgs sectors*, Ph.D. Thesis, UC, Santa Cruz (1999) [hep-ph/9906332] [INSPIRE].